

Note then that the trace of an antilinear operator is undefined, for it is not basis independent: For instance, $\int dq \langle q | \hat{A} q \rangle = \int dq \langle q | \hat{A} \check{Q} q \rangle = \int dq \langle q | \hat{A} | q \rangle = \text{Tr } \hat{A}$, while $\int dp \langle p | \hat{A} p \rangle = \int dp \langle p | \hat{A} | -p \rangle \neq \text{Tr } \hat{A}$.

VI. CONCLUSION

The introduction of a complex conjugator C acting (only) on c numbers renders the manipulation of antilinear operators within Dirac's bra-ket notation as simple as that of linear operators. One just needs to follow the operational rules (α any c number)

$$\check{\alpha} = \alpha^* \check{A}, \quad \langle \psi | \check{A} = C \langle \check{A}^\dagger \psi |, \quad \check{A} | \psi \rangle = | \check{A} \psi \rangle C, \quad (23)$$

with $C\alpha = \alpha^* C$ and $CC=1$, in addition to $\check{A}(|\phi\rangle + |\psi\rangle) = \check{A}|\phi\rangle + \check{A}|\psi\rangle$. To Hermitian conjugate a string of symbols, reverse the order of multiplication, and conjugate each term, using $C^\dagger = C$.

ACKNOWLEDGMENT

I thank Professor Jean LeTourneux for reading the manuscript and suggesting several improvements in the presentation.

¹E. P. Wigner, *Group Theory* (Academic, New York, 1959).

²A. Messiah, *Quantum Mechanics* (North-Holland, Amsterdam, 1958), Chap. XV, Sec. 1.

³P. A. M. Dirac, *The Principles of Quantum Mechanics*, 4th ed. (Oxford University, London, 1958).

⁴A. Royer, "Galilean space-time symmetries in Liouville space and Wigner-Weyl representations," *Phys. Rev. A* **45**, 793-810 (1992).

⁵See, e.g., E. Prugovecki, *Quantum Mechanics in Hilbert Space* (Academic, New York, 1971).

⁶Alternatively: $\langle \phi | \check{A} | \psi \rangle = \langle \phi | \check{A} \psi \rangle C = C \langle \check{A} \psi | \phi \rangle = \langle \psi | \check{A}^\dagger | \phi \rangle$.

⁷ $\int dq |q\rangle C \langle q| = \int dq \int dp |q\rangle C \langle q|p\rangle \langle p| = \int dq \int dp |q\rangle \langle q|-p\rangle C \langle p| = \int dp | -p\rangle C \langle p|$, since $\langle q|-p\rangle = \langle q|p\rangle^*$.

Spectroscopic measurement of the semiconductor energy gap

A. Sconza and G. Torzo

Dipartimento di Fisica Galileo Galilei, Università di Padova, via Marzolo 8, 35131 Padova, Italy

(Received 18 October 1993; accepted 3 February 1994)

A homemade grating spectrometer and simple electronics allow measurements of the energy gap of semiconductor samples in introductory laboratory courses. Both transmission spectra and "photoconductive effect" spectra may be obtained. Results for Ge, Si, GaAs, and InP are reported.

I. INTRODUCTION

The theory of electron energy bands¹ is of paramount importance in the comprehension of the properties of solid matter, and therefore the measurement of the band gap E_g may be considered an essential step in an experimental approach to solid state physics. The present authors previously proposed a simple apparatus for measuring E_g from a plot of resistivity versus temperature,² in bulk semiconductor samples. The same³ and other authors described tutorial experiments to derive E_g from measurements of the temperature dependence of the forward voltage drop⁴ or of the inverse current⁵ in a PN junction. All these methods involve the electron-hole pair production by *thermal excitation*, and they yield a value for E_g^0 , the energy gap *extrapolated at zero kelvin*, by assuming a linear dependence for $E_g(T)$: $E_g(T) = E_g^0 - \alpha T$.

In the present paper we propose a simple apparatus for spectroscopic measurements that can be easily used in an undergraduate laboratory to obtain E_g at *room temperature*. In contrast to the previous ones, this experiment involves electron-hole pair production by *optical excitation*, i.e., by internal photoelectric effect.

The required items are: an inexpensive homemade grating spectrometer equipped with a commercial lamp, two ordinary glass lenses, a low-cost pyroelectric sensor, and simple electronics.

The experiment may be performed either as a measurement of the intensity spectrum of the light transmitted by the semiconductor sample (named *transmission spectrum* thereof) or as a measurement of the photoconductive spectrum, i.e., a plot of the change of the electrical resistance as a function of light wavelength (named *absorption spectrum* thereof).

By performing simultaneously the two measurements the student will grasp a better comprehension of the whole physical process. It will be clear that, for photon energies below E_g , no photon is absorbed because there are no available energy states for the electrons in the forbidden band. As soon as the photon energy reaches E_g an electron in the valence band may be excited into the conduction band, generating an electron-hole pair. Therefore, beside the light absorption, also an increase of the sample electrical conductivity takes place.

The energy gap is measured indeed as the threshold photon energy at which a sharp *increase* of the sample conductivity and a sharp *decrease* of the light transmission occurs. This way of presenting the internal photoelectric effect in semiconductors is somewhat oversimplified because we are not taking into account two second-order effects: the emission or absorption of phonons in the case of indirect-gap transition, and the band tailing in the case of direct-gap transition. This simple picture, however, may be more easily

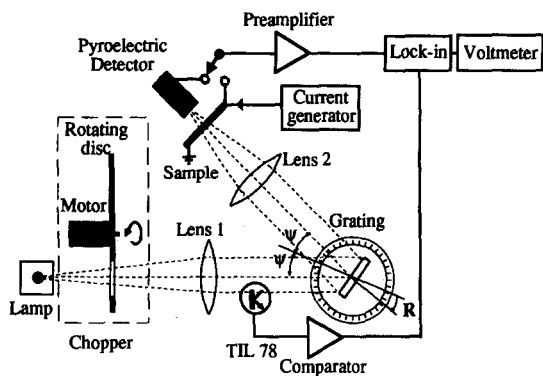


Fig. 1. Experimental setup.

understood by the students, and it is also justified by the limited resolution of our experimental apparatus.

A beautiful and accurate *transmission-only* spectroscopic measurement was recently described by Essick and Mather.⁶ Their more sophisticated approach allows one to distinguish direct and indirect gap transitions, showing also evidence of the exponential band tailing into the forbidden energy gap. Their apparatus however was a professional one, not commonly available in average-equipped didactic laboratories; the apparatus here described, on the other hand, is entirely homemade at low cost and the electronics may be directly built by the students under the teacher's guide. No "black boxes" (such as commercial lock in or monochromator) must be used during the measurements, and the analysis of the results may be performed using the knowledge normally achieved by the students in *introductory* solid state physics courses.

II. EXPERIMENTAL APPARATUS

A block diagram of the experimental setup is reported in Fig. 1. The light source is a commercial prefocused lamp (8 V–50 W) powered by the main ac line through a step-down transformer. A parallel light beam, obtained by a first lens (150 mm focal length), is fed to a reflecting grating,⁷ and the beam is diffracted at a fixed angle 2ψ and focused by a second lens (50 mm focal length) onto the sample. This is a thin semiconductor wafer placed in front of a pyroelectric light sensor⁸ which measures the light transmitted through the sample.

The light wavelength in the diffracted beam can be changed by rotating the grating that is attached to a

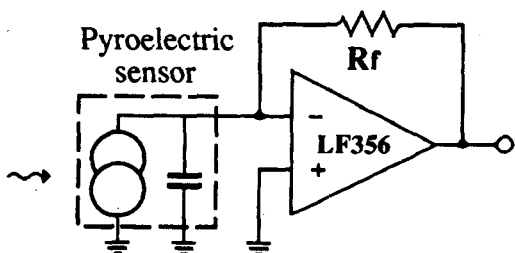


Fig. 2. Current-to-voltage converter for the pyroelectric light sensor.

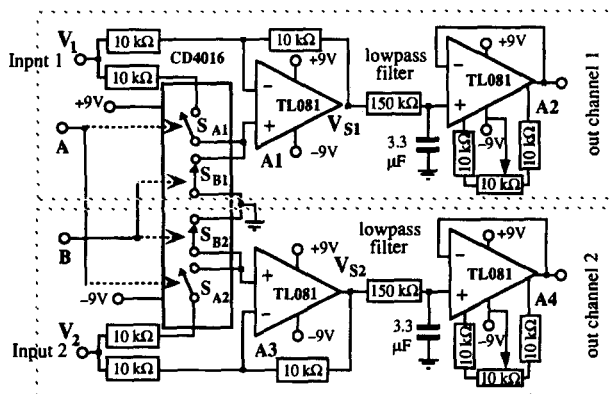
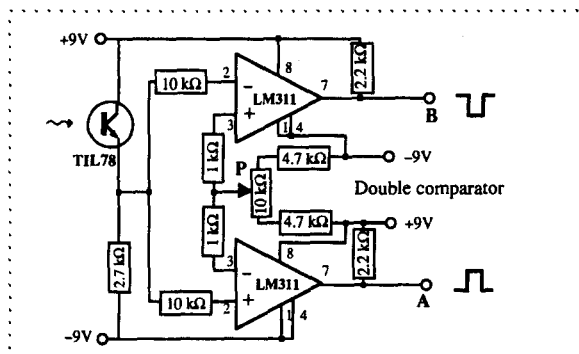


Fig. 3. Homemade double-channel lock-in amplifier. The chopped light, sensed by the phototransistor (TIL78), is converted by a double comparator into square waves (A and B) in phase opposition, that are used as reference signals for the twin-channel lock in. Each channel is made of a synchronous inverter/follower, a low pass filter, and an output buffer, with offset compensation.

goniometer.⁹ The rotation angle R is measured with respect to the position at which the normal to the grating plane bisects the angle 2ψ between the incident and the diffracted beam (i.e., detector on zero-order spectrum).

The wavelength λ of the light reaching the sample for each value of the angle R may be calculated from the diffraction grating dispersion law, in terms of the known value d of the grating spacing and of the constant value of the angle ψ :

$$\lambda(R) = (2/m)d \cos \psi \sin R, \quad (1)$$

where $m=1,2,3,\dots$ is the order of the spectrum.

When λ is measured in μm , the photon energy E is given in eV by the relation $E = hc/\lambda \approx 1.24/\lambda$, where h is the Planck constant and c is the speed of light.

From relation (1) one sees that, at any given angle R , the detector senses more than a single wavelength, i.e., besides the first-order $\lambda_1 = 2d \cos \psi \sin R$ also the second-order $\lambda_2 = d \cos \psi \sin R = \lambda_1/2$, the third-order $\lambda_3 = \lambda_1/3$, etc., normally with decreasing intensities. In some cases (see below) this complicates somewhat the experiment and it requires using a suitable high pass optical filter in order to cut the higher-order wavelengths.

All the optical elements might be independently supported but the alignment of the optics is made much easier by using a two-arms hinged optical bench,¹⁰ with the grating and the goniometer mounted on the hinge axis.

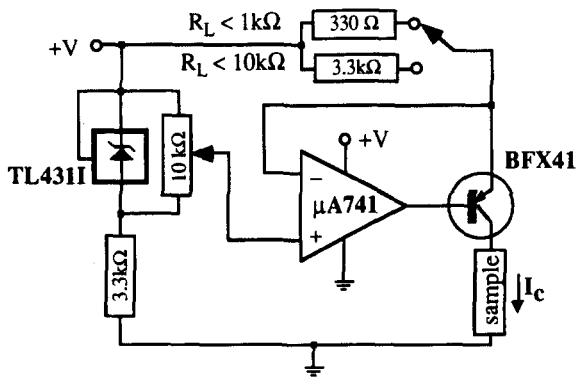


Fig. 4. Constant current generator: the current I_c supplied to the sample is adjusted by the potentiometer, and the low(high) series resistor is chosen for low(high) value of the sample resistance R_L .

The pyroelectric sensor was mounted, with a current-to-voltage converter (Fig. 2), inside a metal can in order to reduce the noise pick up. The pyroelectric current signal is converted into a voltage signal by a single FET-input operational amplifier (LF356) with a large feedback resistance $R_f(2 \times 10^9 \Omega)$, producing an output signal of the order of a few mV, when illuminated by monochromatic light.

An advantage of the pyroelectric sensor, with respect to other light sensors, is a *flat response* over a wide wavelength range. On the other hand it does require a chopped light beam, being sensitive only to the temperature changes produced by the absorbed light. We used therefore a homemade chopper, obtained from a rotating perforated disk that was driven by a turntable dc motor. The light modulation frequency f_0 was about 30 Hz.

With a modulated signal a strong improvement of the signal-to-noise ratio is allowed by using a lock-in technique. A detailed explanation of the principles of phase-lock amplification is not commonly taught in electronics courses, probably owing to the fact that the commercially available lock-in amplifiers are expensive and sophisticated instruments. Nevertheless this powerful technique may be afforded by students too, as previously shown by other authors in this

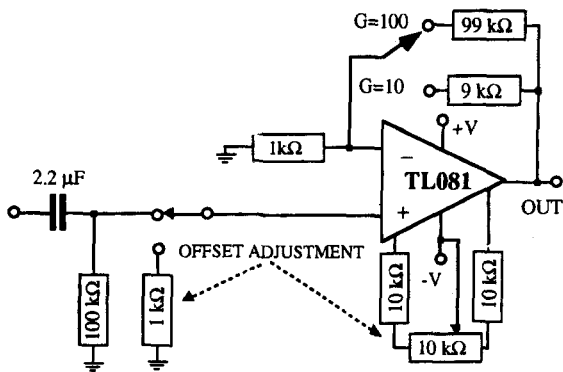


Fig. 5. Noninverting preamplifier with a high-pass filter input stage.

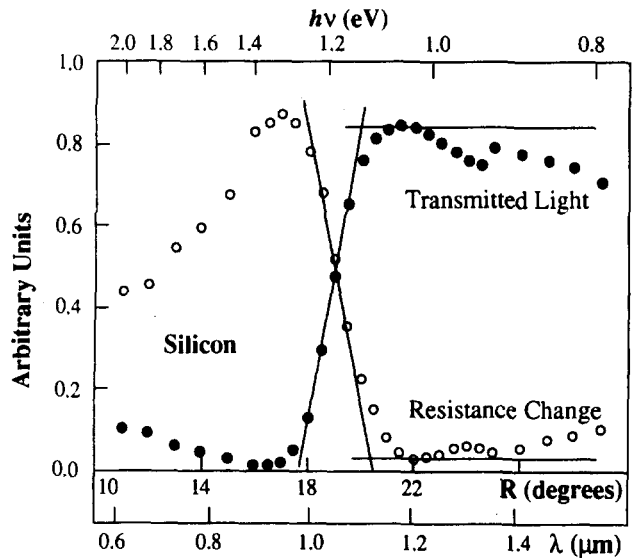


Fig. 6. Absorption and transmission spectra for silicon sample. Black dots: transmission spectrum, measured as ratio between the pyroelectric signal produced by the light transmitted through the sample and the same signal without sample. White dots: absorption spectrum, measured as resistance change of the illuminated sample.

Journal.¹¹ We successfully used for this experiment the very simple version described in Fig. 3, which may be easily built at a negligible cost by using popular integrated circuits.

The synchronous reference signal is taken after the chopper and the first lens by a TIL 78 phototransistor that triggers a double comparator (LM311) whose outputs A and B, in phase opposition, drive two analog switches (CD4016) to toggle the gain of both the amplifiers A1 and A3 between $G = +1$ and $G = -1$. The dc outputs of the two-channel lock in are obtained by filtering out the low-frequency components of V_{S1} and V_{S2} , through low-pass filters (with $RC \gg 1/\omega_0$), and by lowering the output impedance with the buffer stages A2 and A4.

The semiconductor sample is biased by a constant current generator (Fig. 4), so that the resistance change is measured as a change of the voltage signal across the sample. When a two-contacts configuration is adopted, as in our case, one implicitly assumes that the contact resistance is constant during the measurements: this is a good approximation when the contact regions are shaded from the light beam. Both the pyroelectric and the sample photoconductive signals are fed to a high-pass filter (with $RC \gg 1/\omega_0$) at the input stage of a simple noninverting preamplifier whose gain may be set at $G = 10$ or $G = 100$ (Fig. 5).

III. DATA COLLECTION AND ANALYSIS

The semiconductor samples needed in this experiment are slices of approximately $5 \times 20 \text{ mm}^2$ cut from commercial wafers¹² of thickness ranging from 300 to 500 μm . For the transmission measurements they do not require any other preparation, while for the absorption measurement it is necessary to make ohmic contacts at the sample ends. The *absorption* spectrum is obtained in fact by feeding a constant

current through the sample, and measuring the change of the voltage drop across the sample due to the light absorption.

In the case of Ge good ohmic contacts are easily obtained using tin solder. For Si and GaAs samples it is better to evaporate a thin aluminum or gold layer onto the sample ends and then to glue thin copper wires by means of silver epoxy. For the InP sample the contacts were soldered with In.

The measurements are taken in three steps.

(1) We place the semiconductor sample, biased by the constant current generator, in front of the pyroelectric sensor box and we measure the resistance changes (absorption spectrum) as a function of the grating rotation angle R , both for clockwise and anticlockwise rotation; comparing clockwise and anticlockwise spectra gives a check of the correct optical alignment.

(2) We measure the pyroelectric signal due to the light transmitted by the semiconductor wafer (transmission spectrum); first and second step can be performed in a single run if a lock in with two channels similar to the one we presented in Fig. 3 is available.

(3) We remove the semiconductor sample and we measure the pyroelectric signal due to the incident light as a function of the rotation angle R : this spectrum is used to normalize both the transmission and the absorption spectra.¹³

When normalizing the measured spectra, we should take into account the intensity of the light reflected by the semiconductor sample. This can be done approximately by assuming a constant reflection coefficient $r = [(n-1)/(n+1)]^2$ where n is a mean refraction index in the wavelength region of interest, i.e., by neglecting the wavelength dependence of n . The value of r (typically ≈ 0.3), as far as it may be assumed to be constant, does not affect the results of our measurements.

As an example we report in Fig. 6 the results obtained with a Si sample using a grating of 600 lines per mm with an angle $\psi = 15^\circ$. The data are normalized to the light intensity, and they are plotted in arbitrary units as a function of the rotation angle R [which can be converted to the wavelength λ by formula (1) with $m=1$], with a relative scale factor that equates the maxima of both curves.

As expected we see that increasing the photon energy $h\nu$ (i.e., decreasing the rotation angle R), both the transmitted light and the sample conductivity remain nearly constant up to a threshold energy at which both the sample optical absorption and electrical conductivity increase sharply.

To evaluate the energy gap, i.e., the *minimum* value of the photon energy that produces an electron-hole pair, we must obtain from these plots the corresponding *maximum* R (or λ) value. We adopted with our students the following simple procedure: we interpolate with straight lines both the falling edge of the absorption spectrum and the rising edge of the transmission spectrum, and we intersect these two lines with two horizontal lines passing, respectively, through the minimum of the absorption spectrum and through the maximum of the transmission spectrum. The intersection points give us two threshold R values, R_{ta} for absorption and R_{tt} for transmission, respectively: $R_{ta} = 20.3 \pm 0.2$ and $R_{tt} = 20.0 \pm 0.2^\circ$.

From these values we get $E_{ga} = 1.1 \pm 0.01$ eV and $E_{gt} = 1.126 \pm 0.010$ eV. From now on we will quote as final result the average of these two values with an error equal to the half-difference of these values. In the previous case we find $E_g = 1.118 \pm 0.008$ eV, in good agreement with the accepted value $E_g = 1.12$ eV.¹⁴ There is one peculiarity of the Si

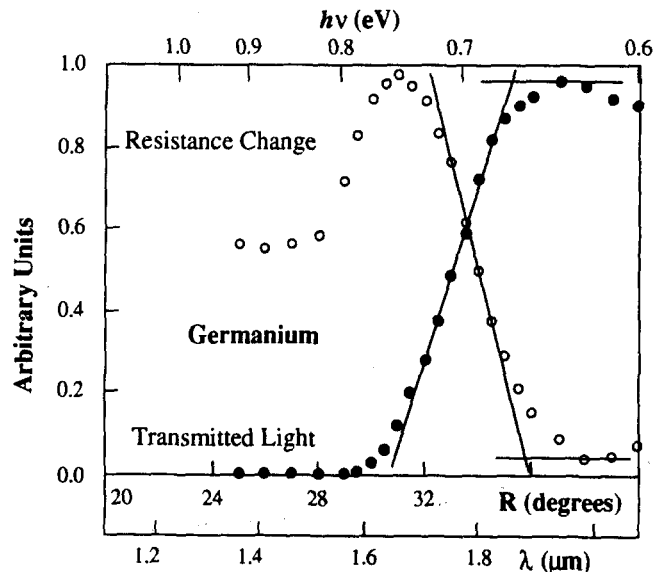


Fig. 7. Absorption and transmission spectra for the germanium sample.

absorption spectrum that requires some comment, i.e., the fact that the normalized spectrum is not flat below the threshold wavelength, as if the short wavelengths (in the visible range and up to $\lambda \approx 0.8-0.9 \mu\text{m}$) were not effective in producing electron-hole pairs. This feature is somewhat confusing for the students, who usually need the teachers' help to get the correct physical explanation. We therefore recall that the light absorption coefficient α in Si is a very rapidly decreasing function of λ ,¹⁵ so that blue light is absorbed in a thickness of the order of $0.1 \mu\text{m}$, while for infrared light with $\lambda \approx 1 \mu\text{m}$ the penetration depth is three orders of magnitude larger. Moreover, at the sample surface there are many re-

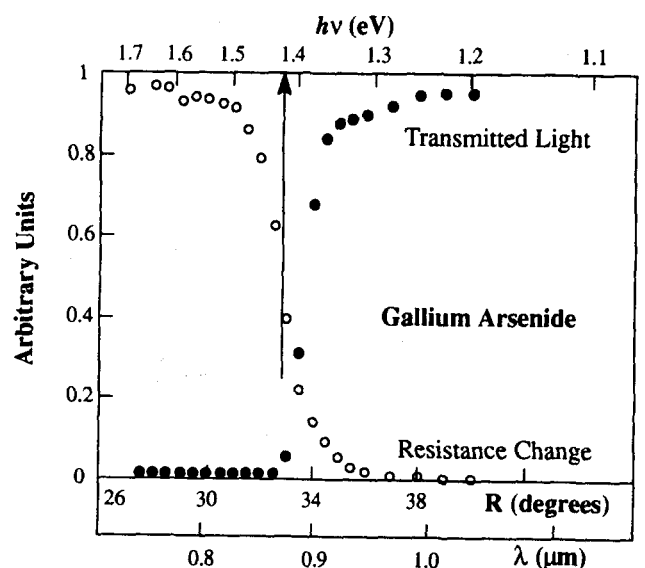


Fig. 8. Absorption and transmission spectra for the gallium arsenide sample: the arrows indicates the accepted value of $E_g = 1.42$ eV.

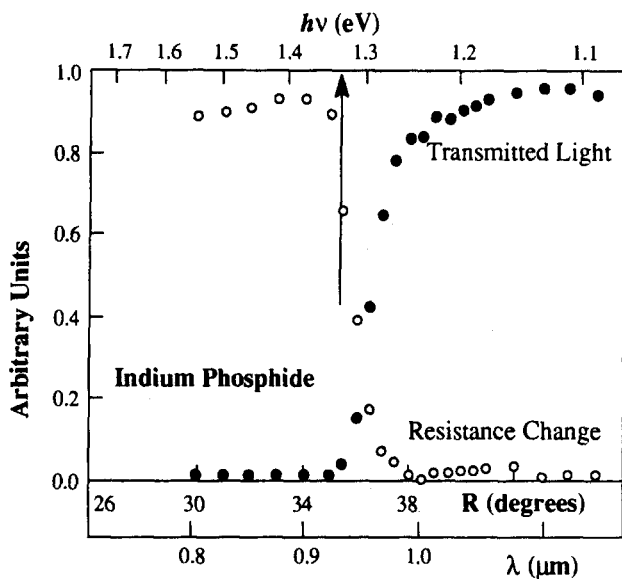


Fig. 9. Absorption and transmission spectra for the indium phosphide sample: the arrow indicates the accepted value of $E_g = 1.33$ eV.

combination centers due to the presence of lattice defects, e.g., those produced by the cutting operation. As a consequence the electron-hole pairs produced at the surface, by the short wavelengths, recombine much more quickly (thus giving no sensible resistance change) than those produced in the bulk by infrared light.

Another consequence of this fact is helpful for our experiment: the visible light of the second- and third-order spectra do not mask the falling edge of the absorption spectrum (practically we do not see other maxima for wavelengths larger than the threshold one). In the case of the Ge samples the situation is less beneficial from this point of view, so that it is convenient to cut all the *visible* light by means of a suitable infrared filter, e.g., the previously used silicon wafer.

In Fig. 7 we report the absorption and transmission spectra obtained with the same diffraction grating and ψ value, a Ge sample, and a Si filter.

We found $R_{tt} = 35.1 \pm 0.2^\circ$ and $R_{ta} = 35.8 \pm 0.2^\circ$, so that we estimate the energy gap to be $E_g = 0.664 \pm 0.006$ eV, which is comparable with the accepted value $E_g = 0.67$ eV, within the estimated error.

The same spectra, obtained without the silicon filter, would be much less readable due to the second-order wavelengths near $0.9 \mu\text{m}$.

The simple method we used to analyze the data obtained for Ge and Si (IV group semiconductors) when applied to the semiconductors of the III-V group gives less correct results. In Fig. 8 we present the spectra obtained with a GaAs sample, with a grating spacing of $0.833 \mu\text{m}$, $\psi = 15^\circ$, and an infrared filter.¹⁶ The threshold angles, defined as before, are: $R_{tt} = 34.4 \pm 0.2^\circ$ and $R_{ta} = 34.0 \pm 0.2^\circ$, that give $E_g = 1.37 \pm 0.01$ eV notably less than the value of 1.42 eV commonly accepted for GaAs.¹⁷

Similarly for an InP sample ($d = 0.833 \mu\text{m}$, $\psi = 15^\circ$, filter RG715) we found (Fig. 9) $R_{tt} = 37.2 \pm 0.2^\circ$ and $R_{ta} = 36.8 \pm 0.2^\circ$ and from these values we get $E_g = 1.28 \pm 0.01$ eV, to be compared with the accepted value of 1.33

eV. The reason for this systematic underestimation of the energy gap may be justified with the students noting the following two facts.

First we note that the defects and impurities content in III-V semiconductors is generally higher than in Ge and Si, due to the more difficult crystal-growth process. This fact yields to an enhanced photon absorption also for energies *below* the threshold energy, involving electrons and holes trapped at impurity energy levels *within* the energy gap (these levels are commonly named *band tail* extending into the forbidden gap).

Second we recall that in direct gap III-V semiconductors, as GaAs and InP, the absorption coefficient in the wavelength region corresponding to the energy gap is much higher ($\alpha \approx 10^4 \text{ cm}^{-1}$) than in group IV semiconductors, like Ge and Si ($\alpha \approx 10 \text{ cm}^{-1}$). In Ge and Si, in fact, the photon absorption requires a two-step process involving a momentum exchange with the crystal lattice (*indirect* process with a phonon absorption or emission),¹⁸ and therefore it has lower probability than in direct-gap semiconductors. The light intensity after a sample of ≈ 0.5 mm thickness and with an absorption coefficient of $\approx 10^4 \text{ cm}^{-1}$ is too low to allow us to measure accurately the light transmission close to E_g .

For these reasons we suggest to our students the following "rule of thumb" for calculating an *approximate value* of the energy gap for the GaAs and InP samples: to assume as "threshold wavelength" the mean value of the interval of wavelengths where the absorption spectrum falls down and the transmission spectrum rises to a maximum value. This partially accounts for the downward shift of the measured threshold energy due to the band tail.

Using this rule we find for the GaAs sample: $31.7 < R_{ta} < 34.1^\circ$ and $32.7 < R_{tt} < 34.7^\circ$, that averaged and converted to photon energies give $E_g = 1.40 \pm 0.03$ eV. Similarly for the InP sample we find $35.0 < R_{ta} < 36.7^\circ$ and $35.9 < R_{tt} < 37.3^\circ$, i.e., in terms of photon energy an average value $E_g = 1.30 \pm 0.02$ eV.

IV. CONCLUSIONS

The present experiment has been successfully performed by several groups of students in the fourth-year physics laboratory course at the physics department of our university, during the last three academic years. The students were trained to build their experimental setup, to make the measurements, and finally to discuss the results obtained and the performance of their apparatus. Two important advantages of the present approach, from the didactic point of view, are: (i) the ability to show the simultaneous effects of light absorption and of electron-hole pair production, and (ii) the easiness of getting the students familiar with the lock-in technique, which is powerful detection method widely employed in many fields of scientific research, without excessive prerequisites in electronics.

We think that this experiment, despite its obvious limitations in wavelength resolution and minimum detectable light intensity, can be a valuable one in an introductory course where the emphasis is on understanding the basic mechanism of electron-hole pair creation by photons.

ACKNOWLEDGMENTS

We gratefully acknowledge the laboratory LAMEL-CNR (Consiglio Nazionale delle Ricerche) for providing us the major part of the samples used in this experiment.

- ¹C. Kittel, *Introduction to Solid State Physics*, 5th ed. (Wiley, New York, 1976).
- ²A. Sconza and G. Torzo, "An undergraduate laboratory experiment for measuring the energy gap in semiconductors," *Eur. J. Phys.* **10**, 123–126 (1989); see also J. N. Fox and N. W. Gaggini, "A computer interfaced experiment to measure the electrical resistivity of a semiconductor," *ibid.* **8**, 273–276 (1987).
- ³A. Sconza, G. Torzo, and G. Viola, "Experiment on the physics of the PN junction," *Am. J. Phys.* **62**, 66–70 (1994).
- ⁴Y. Canivez, "Quick and easy measurement of the band gap in semiconductors," *Eur. J. Phys.* **4**, 42–44 (1983); L. Kirkup and F. Placido, "Undergraduate experiment: determination of the band gap in germanium and silicon," *Am. J. Phys.* **54**, 918–920 (1986); L. Kirkup and M. Nicolson, "Band-gap measurements based upon the behavior of a *p-n* junction," *Eur. J. Phys.* **7**, 49–51 (1986).
- ⁵P. J. Collings, "Simple measurement of the band gap in silicon and germanium," *Am. J. Phys.* **48**, 197–199 (1980).
- ⁶J. M. Essick and R. T. Mather, "Characterization of a bulk semiconductor's band gap via a near-absorption edge optical transmission experiment," *Am. J. Phys.* **61**, 646–649 (1993).
- ⁷Good quality low-price (less than \$100) grating may be purchased from Edmund Scientific. We used the model 41028, 600 lines/mm, blaze wavelength 0.5 μm , and the model 41037, 1200 lines/mm.
- ⁸ELTEC Instruments, Inc. P. O. Box 9610 Central Business Park, Daytona Beach, FL, model 400: sapphire window, 2 mm^2 sensing area, sensitivity 600 V/W (or 1.2 $\mu\text{A}/\text{W}$), risetime 0.2 ms, optical bandwidth 0.2–4 μm , (price \approx \$50).
- ⁹A cheap goniometer, that gives a resolution of about 0.5°, may be obtained from a plastic tool used for measuring angles in technical drawing.
- ¹⁰The rails length of our optical bench is 70 cm: with a 6 mm wide slit in front of the second lens we have a resolution $\Delta\lambda \approx 0.02 \mu\text{m}$ using the first order spectrum.
- ¹¹R. Wolfson, "The lock-in amplifier: A student experiment," *Am. J. Phys.* **59**, 569–572 (1991); P. A. Temple, "An introduction to phase-sensitive amplifiers: An inexpensive student instrument," *ibid.* **43**, 801–807 (1975); A very useful, exhaustive tutorial textbook on this topic is M. L. Meade *Lock-in Amplifiers: Principles and Applications* (Peregrinus, London, 1983).
- ¹²Germanium and silicon wafers of various thickness and resistivity may be purchased from Metallurgie Hoboken Overpelt, Hoboken, Belgium, or from BDH Chemicals Ltd, London, UK. GaAs and InP wafers are produced by many industries, e.g., MCP Wafer Technology Ltd., Milton Keynes, UK, or Nippon Mining Co. Ltd., Tokyo, Japan, or by Sumitomo Electric industries, Hyogo, Japan. For the measurements here reported we used the following samples (t =thickness, l =length, w =width, ρ =resistivity, R =resistance). Silicon: $t=0.0385 \text{ cm}$, $l=1.3 \text{ cm}$, $w=0.5 \text{ cm}$, $\rho \approx 100 \Omega \text{ cm}$, $R \approx 8 \text{ k}\Omega$; germanium: $t=0.043 \text{ cm}$, $l=1.3 \text{ cm}$, $w=1.1 \text{ cm}$, $\rho \approx 45 \Omega \text{ cm}$, $R \approx 1.2 \text{ k}\Omega$; gallium arsenide: $t=0.05 \text{ cm}$, $w=l=1 \text{ cm}$, $\rho \approx 1000 \Omega \text{ cm}$, with two gold plated dots placed at diagonally opposed corners, $R \approx 30 \text{ k}\Omega$; indium phosphide: $R \approx 4 \text{ k}\Omega$, $t \approx 2 \mu\text{m}$ layer onto a 0.4 mm-thick semi-insulating InP(Fe-doped) substrate, $w=l=1 \text{ cm}$, $\rho \approx 1 \Omega \text{ cm}$, with two In-soldered contacts.
- ¹³The shape of the measured spectra in fact depends on several factors: the lamp emission spectrum, the grating chromatic efficiency, the lens absorption coefficient.
- ¹⁴O. Madelung, *Semiconductors: Group IV Elements and III-V Compounds, in Data in Science and Technology*, edited by R. Poerschke (Springer, Berlin, 1991).
- ¹⁵The absorption coefficient α is defined by the relation $I=I_0 \exp(-\alpha x)$, where I_0 and I are the incident and transmitted light intensity at depth x . The α values for the most common semiconductors may be found for example in S. M. Sze, *Physics of Semiconductor Devices* (Wiley, New York, 1969), Chap. 12, paragraph 4.2.
- ¹⁶Model RG 715 by Newport Instruments AG; threshold wavelength 0.715 μm .
- ¹⁷The same threshold energy value was found for the absorption edge in GaAs by J. M. Essick and R. T. Mather (see Ref. 6).
- ¹⁸See C. Kittel, Ref. 1, Chap. 10. A detailed analysis of this indirect-gap absorption process, given by G. G. Macfarlane, T. P. McLean, J. E. Quarington, and V. Roberts, ["Fine structure in the absorption-edge spectrum of Si," *Phys. Rev.* **111**, 1245–1254 (1958)], shows that the momentum-conserving phonon energy is much less than the photon energy (of the order of some percent): neglecting the phonon energy we underestimate E_g of the same amount.

Products of rotations: A geometrical point of view

Jean Sivardière

CEA/Département de Recherche Fondamentale sur la Matière Condensée/SPSMS/LIH, 38054 Grenoble Cedex 9, France

(Received 1 November 1993; accepted 24 March 1994)

Products of rotations can be studied by a very simple and concise geometrical method based on the decomposition of a rotation into two mirror operations: use of dyadics, quaternions, or even matrices is not necessary. The Rodrigues formulas are derived. Products of finite order rotations and Euler rotations are considered.

I. INTRODUCTION

The product of two rotations around intersecting axes was studied by Euler as early as 1775, and finally derived independently by Gauss (1819, published only in 1863), Rodrigues (1840), Hamilton and Cayley (1845) (see Refs. 1 and 2 for detailed historical reviews and interesting references). Various approaches are now available to determine such a product: the dyadic description of rotations introduced by Gibbs and Heaviside about 1880, and their corresponding vectorial representation by the matrices of the orthogonal group $\text{SO}(3)$ or D_1 ; ^{3–5} the description of rotations by Hamil-

ton quaternions, and their corresponding spinor representation by the Pauli matrices of the group $\text{SU}(2)$ or $D_{1/2}$, the elements of which are the Cayley–Klein parameters, and which was introduced by Cartan using the stereographic projection; ^{1,3,6} a purely geometrical approach initiated by Euler and brilliantly developed by Rodrigues, which has been illustrated by the so-called Euler–Rodrigues construction ^{1,7,8} and more recently by the Biedenharn–Louck representation of rotations by “turns,” or ordered pairs of points on the surface of the unit sphere. ^{9,10}

In this paper, we review the product of rotations from an